

A photometric selection of White Dwarf candidates in SDSS DR10

Nicola Pietro Gentile Fusillo¹, Boris T. Gänsicke¹, Sandra Greiss¹

¹ *Department of Physics, University of Warwick, Coventry, CV4 7AL, UK*

4 March 2022

ABSTRACT

We present a method which uses cuts in colour-colour and reduced proper motion-colour space to select white dwarfs without the recourse to spectroscopy while allowing an adjustable compromise between completeness and efficiency. Rather than just producing a list of white dwarf candidates, our method calculates a *probability of being a white dwarf* (P_{WD}) for any object with available multi band photometry and proper motion. We applied this method to all objects in the SDSS DR10 photometric footprint and to a few selected sources in DR7 which did not have reliable photometry in DR9 or DR10. This application results in a sample of 61969 DR10 and 3799 DR7 photometric sources with calculated P_{WD} from which it is possible to select a sample of ~ 23000 high-fidelity white dwarf candidates with $T_{\text{eff}} \gtrsim 7000$ K and $g \leq 19$. This sample contains over 14000 high confidence white dwarfs candidates which have not yet received spectroscopic follow-up. These numbers show that, to date, the spectroscopic coverage of white dwarfs in the SDSS photometric footprint is, on average, only $\sim 40\%$ complete. While we describe here in detail the application of our selection to the SDSS catalogue, the same method could easily be applied to other multi colour, large area surveys. We also publish a list of 8701 bright ($g \leq 19$) WDs with SDSS spectroscopy, of which 1781 are new identifications in DR9/10.

Key words: white dwarfs-surveys-catalogues

1 INTRODUCTION

White dwarfs (WD) are the stellar remnants left over from the evolution of stars with main sequence masses $M > 0.8M_{\odot}$ and $M \lesssim 8 - 10M_{\odot}$ (Iben et al. 1997, Smartt et al. 2009, Doherty et al. 2015). This mass range includes over 90% of all the stars in the Galaxy, making white dwarfs by far the most common stellar remnants. Large samples of white dwarfs are required to reliably constrain fundamental parameters such as space density (Holberg et al. 2002, Holberg et al. 2008, Giammichele et al. 2012, Sion et al. 2014), mass distribution (Bergeron et al. 1992, Liebert et al. 2005, Kepler et al. 2007, Falcon et al. 2010, Tremblay et al. 2013, Kleinman et al. 2013) and luminosity function, which in turn can be used to determine the ages of the individual Galactic populations (Oswalt et al. 1996, De Gennaro et al. 2008, Cojocaru et al. 2014).

Furthermore, well defined large samples of white dwarfs are an extremely useful starting point for identifying rare white dwarf types like magnetic white dwarfs (Gänsicke et al. 2002, Schmidt et al. 2003, Külebi et al. 2009, Kepler et al. 2013), pulsating white dwarfs (Castanheira et al. 2004, Greiss et al. 2014), high/low

mass white dwarfs (Vennes & Kawka 2008, Brown et al. 2010, Hermes et al. 2014), white dwarfs with unresolved low mass companions (Farihi et al. 2005, Girven et al. 2011, Steele et al. 2013), white dwarfs with rare atmospheric composition (Schmidt et al. 1999, Dufour et al. 2010, Gänsicke et al. 2010), close white dwarf binaries (Marsh et al. 2004, Parsons et al. 2011), metal polluted white dwarfs (Sion et al. 1990, Zuckerman & Reid 1998, Dufour et al. 2007, Koester et al. 2014) or white dwarfs with dusty or gaseous planetary debris discs (Gänsicke et al. 2006, Farihi et al. 2009, Debes et al. 2011, Wilson et al. 2014). Because of their intrinsic low luminosities identifying a large, complete and well defined sample of white dwarfs still remains a challenge. Much progress has been made in recent years thanks to large area surveys, first and foremost the Sloan Digital Sky Survey (SDSS, York et al. 2000) (Harris et al. 2003, Eisenstein et al. 2006, Kleinman et al. 2013). The largest published catalogue of white dwarfs to date (Kleinman et al. 2013) fully exploited the spectroscopic data available at the time of SDSS data release 7 and contains over 20000 white dwarfs (of which 7424 with $g \leq 19$). However not only is DR7 now outdated, but SDSS spectroscopy is only available for less than 0.01%

of all SDSS photometric sources. Furthermore most of SDSS's white dwarfs are only serendipitous spectroscopic targets. The true potential of SDSS's vast multi band photometric coverage still remains to be fully mined for white dwarf research, but this requires a reliable method able to select white dwarfs candidates without recourse to spectroscopy. Proper motion has been traditionally used to distinguish white dwarfs from other stellar populations. In particular many studies that contributed to the census of white dwarfs in the solar neighbourhood specifically targeted high proper motion objects (Holberg et al. 2002, Sayres et al. 2012, Limoges et al. 2013). In this paper we present a novel method which makes use of photometric data and proper motions to calculate a *probability of being a WD* (P_{WD}) for any photometric source within a broad region in colour space. Unlike any previous similar work, our method does not use a specific cut in colour or proper motion to generate a list of white dwarf candidates; instead it provides a catalogue of sources with an associated P_{WD} . These P_{WD} can then be used to create samples of white dwarf candidates best suited for different specific uses. By applying our method to the full photometric footprint of SDSS DR10, we created a catalogue which includes ~ 23000 bright ($g \leq 19$) high-fidelity white dwarfs candidates. Using this catalogue, we assess the spectroscopic completeness of the SDSS white dwarf sample.

2 SDSS

The Sloan Digital Sky Survey has been in continuous operation since 2000. It uses a dedicated 2.5 meter telescope at Apache Point in New Mexico to carry out multi band photometric observation of the northern sky and follow-up spectroscopy of selected targets. We have made use of the SDSS Data Release (DR) 7 (Abazajian et al. 2009), DR9 (Ahn et al. 2012) and DR10 (Ahn et al. 2014), which are, respectively, the last DR of the SDSS-II project and the second and third DRs of the SDSS-III project. All data releases provide *ugriz* photometry spanning a magnitude range $\sim 15 - 22$ and proper motions computed from the USNO-B and SDSS positions. In the sample we examined as part of this work there is no object with a measured proper motion exactly equal to zero, but $\simeq 2\%$ of objects with magnitude $g \leq 19$ have no proper motion in the SDSS database. This is probably because these objects did not have a reliable match on the USNO-B photographic plates. From here on we will refer to these objects as having no proper motion, even though their proper motions have, probably, simply not been computed and are actually not zero in value. SDSS DR7 includes photometric coverage of 11500 deg^2 and follow-up low-resolution ($R \simeq 1850 - 2200, 3800 - 9200 \text{ \AA}$) spectroscopy for 1.44 million galaxies, quasars, and stars. In SDSS DR9 the photometric sky coverage was extended to a total 14555 deg^2 which includes 2500 deg^2 in the Southern Galactic Cap (Fig. 1). In SDSS-III a new improved spectrograph called BOSS is used providing larger wavelength coverage ($3600 - 10400 \text{ \AA}$ Ahn et al. 2012) as well as higher spectral resolution ($R \simeq 1560 - 2650$). As of DR10 Sloan released over 3.35 million useful optical spectra.

Even though the main targets of BOSS spectroscopic follow-up are quasars and galaxies, about 3.5% of the BOSS fibers

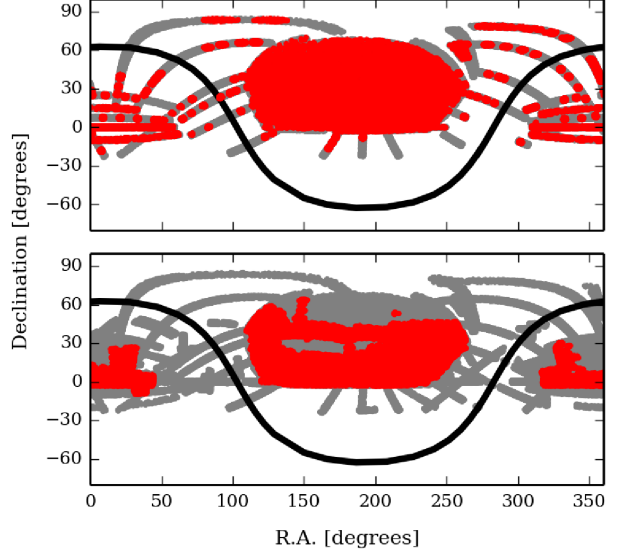


Figure 1. Photometric coverage (grey) of SDSS DR7 (top panel) and SDSS DR10 (bottom panel) in equatorial coordinates. The spectroscopic coverages of the SDSS-II spectrograph for DR7 and BOSS for DR10 are overlaid in red. The black line indicates the location of the galactic plane.

Table 2. Equations describing the colour and magnitude constraints used to select primary sources in the SDSS footprint.

Colour	constraint	
$(u - g)$	\leq	$3.917 \times (g - r) + 2.344$
$(u - g)$	\leq	$0.098 \times (g - r) + 0.721$
$(u - g)$	\geq	$1.299 \times (g - r) - 0.079$
$(g - r)$	\leq	0.450
$(g - r)$	\geq	$2.191 \times (r - i) - 0.638$
$(r - i)$	\leq	$-0.452 \times (i - z) + 0.282$
g	\leq	19
$type$	$=$	6

in DR9 and DR10 were devoted to a series of 25 small ancillary projects. Particularly relevant to our work is the white dwarf and hot subdwarf ancillary project which targeted ~ 5700 white dwarf and hot subdwarf candidates selected according to their $u - r$, $u - g$, $g - r$ colours (Dawson et al. 2013, Ahn et al. 2014, Sect. 6.3).

3 DEVELOPING A PHOTOMETRIC SELECTION METHOD

We first retrieved spectra, *ugriz* photometry and proper motions for all the primary point sources with available spectra in DR7 within a broad region selected in the $(u - g, g - r)$, $(g - r, r - i)$, and $(r - i, i - z)$ colour-colour planes (Fig. 2, Table 2). The shape and extension of these colour-cuts were defined such that they included all of the objects which had been classified as either spectroscopically confirmed white dwarfs or as photometric white dwarf candidates by Girven et al. (2011). At this stage we were aiming to be as

Table 1. Summary of the most relevant numbers presented in the paper

magnitude limit of the catalogue	$g \leq 19$
Objects in main DR10 photometric catalogue (sect. 5)	61969
Objects in DR7 extension (sect. 7.3)	3799
Objects with DR7 spectra in initial colour cut	28213
Poor quality spectra or no proper motion	574
Objects in DR7 training sample (sect. 3, Table 2)	27639
WDs in the DR7 training sample	6706
Contaminants in the DR7 training sample	20933
Object with SDSS/BOSS spectra in the catalogue	33073
WDs with SDSS/BOSS spectra in the catalogue (Table 4)	8701
High confidence WDs candidates in the catalogue	~ 23000
Of which with no SDSS spectra	~ 14000
WDs from Kleinman et al. (2013) included in our catalogue (sect. 8.1)	6689
Kleinman et al. (2013) WDs not classified as WDs by us	30
Objects with a DR7 spectrum classified by us as WDs, not included in the Kleinman et al. (2013) catalogue	261

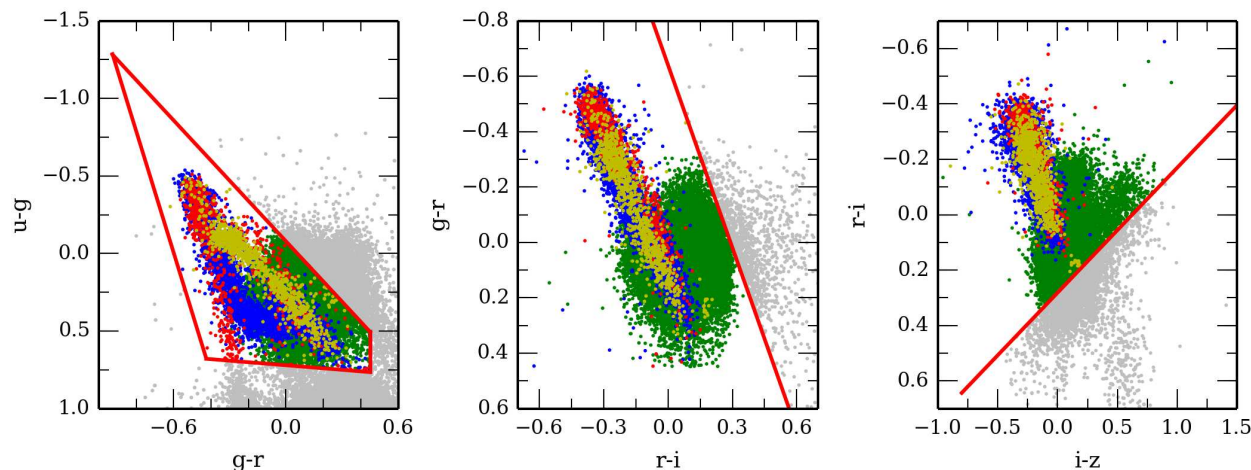

Figure 2. Colour-colour diagrams illustrating the location of the 27639 DR7 spectroscopic objects that we used as training sample for our selection method. DA white dwarfs, non DA white dwarfs, NLHS and quasars are shown as blue, yellow, red and green dots respectively. The colour cuts that define our initial broad selection from Table 2 are overlaid as red lines. Objects outside this selection were not classified and are therefore plotted as grey dots.

Table 3. Classification of the 28213 objects with available spectra and with $g \leq 19$ selected from DR7

Class	number of objects
DA	5271
DB	497
DAB/DBA	95
DAO	49
DC	404
DZ	111
DQ	120
Magnetic WD	134
WD+MS	197
CV	94
NLHS	1454
QSO	19739
Unreliable	36
Unclassified	12

complete as possible and no real effort was made to avoid contamination.

In developing our selection method, we relied on visual classification of our initial spectroscopic sample and on proper motions. Sloan objects fainter than $g \sim 19$ often have noisy spectra and missing or unreliable proper motions. For this reason we decided to limit ourselves to bright sources ($g \leq 19$).

This first sample included 28213 objects which we classified according to spectral appearance. For the development of the selection method we only needed to classify these objects in 3 broad categories: "white dwarfs", "non white dwarfs" and "unreliable" (where the S/N was too low for classification). However we decided that a more detailed classification could help to diagnose biases during the development of the selection method and provide useful statistics. Therefore we subdivided the "white dwarfs" into 10 types (DA, DB, DC, Magnetic white dwarfs,... Table 3) and the "non WDs" into "QSOs" and a second category "Narrow Line Hydrogen Stars" (NLHS, a mixed bag of stars with low-

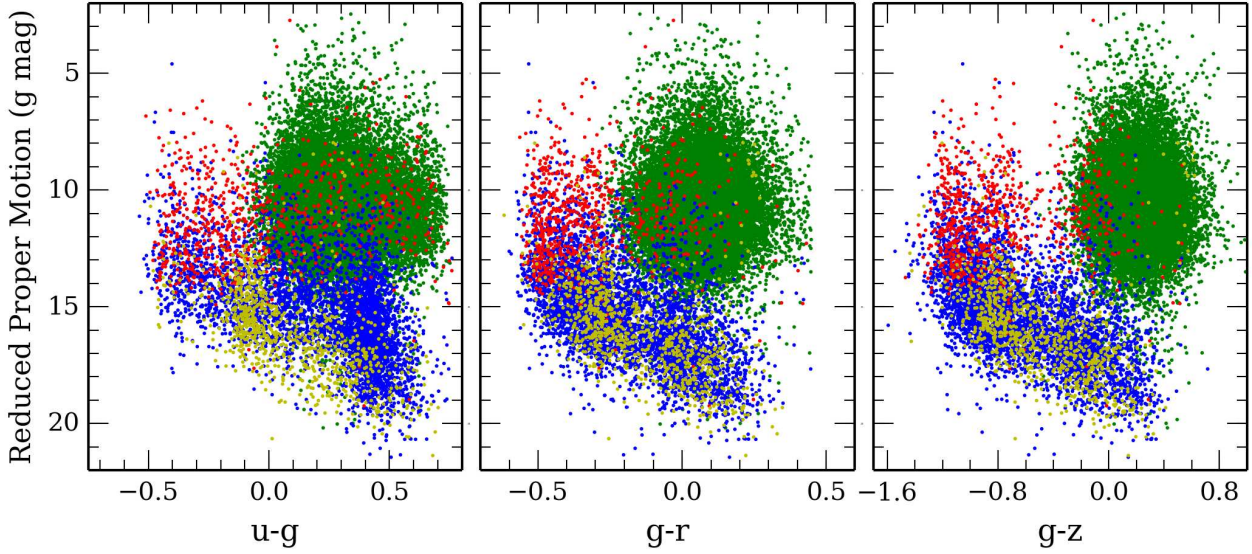


Figure 3. Reduced proper motion-colour diagrams illustrating the location of the 27639 DR7 spectroscopic objects of our training sample (Table 3). DA white dwarfs, non DA white dwarfs, NLHS and quasars are shown as blue, yellow, red and green dots respectively.

gravity hydrogen dominated atmospheres, including subdwarfs, extreme horizontal branch stars and A/B type star). The NLHS sample may include a very small number of extremely low mass (ELM, Brown et al. 2012, Hermes et al. 2014, Gianninas et al. 2014) white dwarfs. However we correctly identified all but one known ELM white dwarfs in our training sample (see Sect. 7.2 for a detailed discussion). The results of our classification are summarized in Table 3.

After discarding 36 objects with “unreliable” spectra, we calculated reduced proper motions (RPMs) for all the objects in the sample,

$$H = g + 5 \log \mu + 5 \quad (1)$$

with the Sloan g magnitude and the proper motion μ in arcsec/year. 538 objects (of which 265 white dwarfs) did not have proper motions, reducing the size of our initial sample to 27639 (Table 1). These 27639 spectroscopically confirmed white dwarfs and contaminants with calculated RPM were the *training sample* on which we developed our selection method. RPM can be used as a proxy for absolute magnitude for a given transverse velocity and, with accurate photometry and astrometry, colour-RPM diagrams can show a very clean separation between main sequence stars, subdwarfs, white dwarfs and quasars.

The training sample was used to trace the loci occupied by white dwarfs and contaminants in RPM colour space and to explore the separation between the two types of objects achieved using different colours. We found that the strongest discrimination between white dwarfs and contaminants is obtained in $(g - z, \text{RPM})$ space which we therefore adopted for our selection method (Fig. 3).

We then mapped the distribution of the white dwarfs and contaminants of our training sample in RPM colour space. In order to create a smooth continuous map, every object was included as a 2D Gaussian the width of which reflects the uncertainty of the RPM and $(g - z)$ colour of the object. The Gaussians were normalised so that their volume

equals unity and therefore the integral over the map is equal to the number of objects in the training sample. In this way we produced a continuous smeared-out “density map” for white dwarfs, and another one for contaminants.

The proper motions computed by SDSS for objects with $g \leq 19$ are accurate to ~ 2.5 mas/year (Ahn et al. 2012), but many objects (most of the QSO) have proper motion values < 2 mas/year and, consequently, large relative uncertainties. These values generate very large uncertainties in the computed RPMs and translate into Gaussians extremely stretched in the RPM dimension. These objects with poor proper motion measurements can, in fact, be smeared over the entire RPM dimension “polluting” even areas which should be populated only by the highest proper motion objects. Furthermore by visually inspecting the $(g - z, \text{RPM})$ distribution of QSO it is instantly obvious that they all cluster in a well defined locus which has a far smaller extension in the RPM dimension than the uncertainties of these low proper motions. To avoid such artifacts affecting our maps we decided to limit the maximum uncertainty in proper motion for any object to one third of the proper motion value. This correction only affects the objects with the lowest proper motions which, in the case of our training sample, are ~ 10000 QSOs and ~ 200 other contaminants.

We then defined a map providing the *probability of being a white dwarf* (P_{WD}), as the ratio of the white dwarf density map to the sum of both density maps (white dwarfs and contaminants). P_{WD} of any given object is calculated by integrating the product of its Gaussian distribution in the $(g - z, \text{RPM})$ plane with the underlying probability map (Fig. 4). For any given photometric source this value directly indicates how likely it is for the source to be a white dwarf. Our DR7 training sample only contained few objects with very high RPMs and therefore the probability map is scarcely populated in the regime of extremely high RPM. This leads to a “patchy” probability map with blank areas with no information. When calculating P_{WD} for objects out-

side our training sample, the blank areas, caused by lack of data, would generate low probability values which would not reflect any actual likelihood of being a white dwarf.

To obviate this problem we decided to define a line in $(g - z, \text{RPM})$ space such that the P_{WD} of all objects below this line is assumed as 1.0. The line, given by

$$\text{RPM} > 2.72 \times (g - z) + 19.19 \quad (2)$$

was defined by inspecting the $(g - z, \text{RPM})$ diagram of the spectroscopic sample and trying to include as much as the sparsely populated area as possible, while minimising the number of contaminants that would undergo such probability correction. (Fig. 4).

Using the calculated P_{WD} it is now possible to make different confidence selections by defining any object with an associated probability above an arbitrary threshold as a white dwarf candidate. When choosing such threshold value, completeness and efficiency are the key parameters one needs to compromise between. Reference values of completeness and efficiency can be calculated using again our training sample. For a given P_{WD} threshold, we define *completeness* as the ratio of the number of white dwarfs in the training sample with at least that associated probability to the total number of white dwarfs in the sample. Similarly *efficiency* is defined as the ratio of the number of white dwarfs selected by the probability cut to the number of all the objects retrieved by such selection. While testing the selection method we determined that we can generate from our DR7 training sample a 95% complete sample with 89.7% efficiency by selecting objects with $P_{\text{WD}} \geq 0.41$ (Fig. 5). Fig. 5 clearly shows that the efficiency of any confidence cut increases sharply up to probability values of ~ 0.08 and more slowly after that. This effect is caused by the fact that the vast majority of the contaminants in our training sample are quasars with $P_{\text{WD}} < 0.1$ while most of the white dwarfs in the training sample have $P_{\text{WD}} > 0.8$. Fig. 6 illustrates the distribution of white dwarfs and contaminants in terms of their P_{WD} and shows that there are indeed only a few objects with probabilities between 0.1 and 0.8. Therefore even if a confidence cut at probabilities of 0.1 already yields an efficiency of $\sim 80\%$, much better completeness-efficiency compromises can be achieved using higher probability thresholds and P_{WD} so low should be chosen only when compiling a catalogue which aims to maximise completeness. Finally, in Fig. 7 we use colour-colour diagrams to further illustrate the reliability of our selection method by comparing the a 95% complete photometric sample with the DR7 spectroscopic training sample.

4 WHITE DWARFS WITH NEW SPECTRA IN DR9/10

Using again the broad selection described in Table 2, we retrieved *ugriz* photometry, proper motions and spectra for 8215 objects which received spectroscopic follow-up after DR7 up as part of SDSS-III. These are predominately objects observed with the BOSS spectrograph, including only 102 targets of the Segue-II program still observed with the old SDSS spectrograph. We classified the spectra by visual inspection (Table 4). The 3560 objects identified as white dwarfs form an independent sample of spectroscopically con-

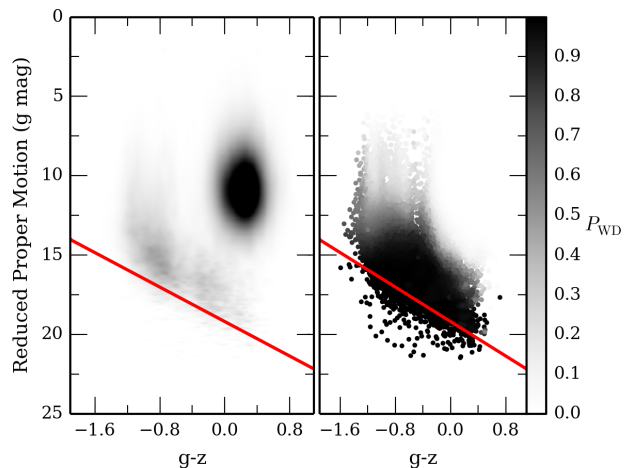


Figure 4. Distribution in $(g - z, \text{RPM})$ of the 27639 white dwarfs and contaminants of the DR7 spectroscopic sample. In the left panel the objects are included as 2D Gaussians to account for the uncertainties in their parameter and the gray-scale reflects the spatial density. In the right panel the grey-scale indicates the calculated P_{WD} with darker objects having higher values than lighter ones. All objects below the red line had their P_{WD} fixed to 1.0

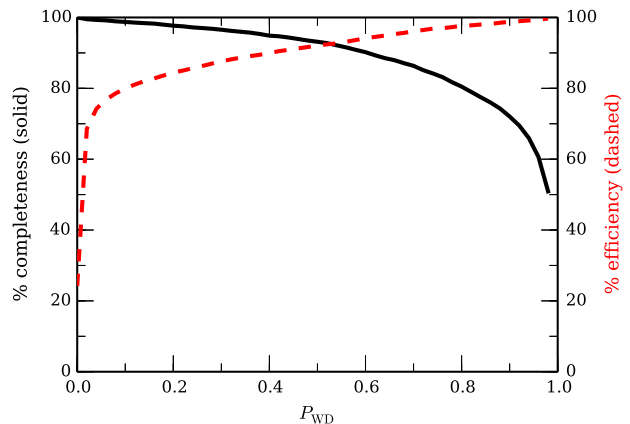


Figure 5. Completeness (solid line) and efficiency (dashed line) of samples of white dwarf candidates from our catalogue shown as functions of the minimum value of P_{WD} an object must have in order to be selected. These values of completeness and efficiency were computed using the spectroscopic DR7 training sample as a reference.

firmed white dwarfs which we used to further test the reliability of our selection method. Furthermore 1752 of these white dwarfs did not have a spectrum prior to DR9 and are therefore new spectroscopically confirmed white dwarfs. We used the $(g - z, \text{RPM})$ probability map to estimate P_{WD} for 3522 of these 3560 white dwarfs (since 38 of them did not have proper motion) and verify that their P_{WD} computed from the DR7 probability map are consistent with the spectroscopic classification. Fig. 8 clearly shows that the vast majority of the white dwarfs with new DR9/10 spectra have $P_{\text{WD}} > 0.6$ and over 80% of spectroscopically confirmed contaminants have $P_{\text{WD}} < 0.1$ confirming that our selection method can reliably distinguish between white dwarfs and

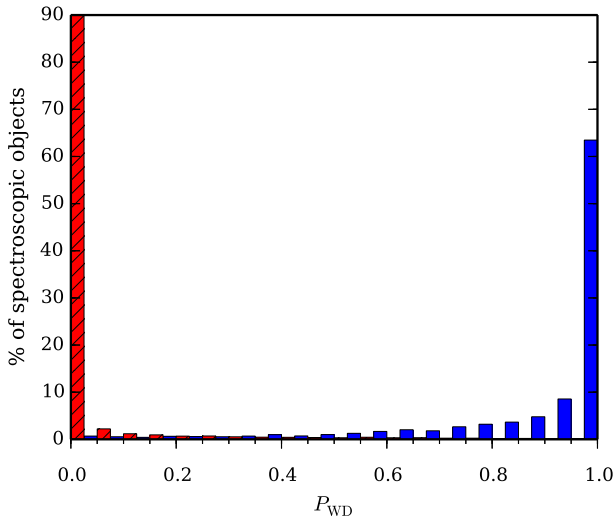


Figure 6. Distribution of 27639 spectroscopically identified white dwarfs (blue) and contaminants (red, shaded) from the DR7 training sample as a function of P_{WD} .

Table 4. Classification of the 8215 objects with spectra taken after DR7, with $g \leq 19$ within the initial broad colour-cut. The new spectroscopically confirmed white dwarfs had not received any spectroscopic follow up before DR9.

Class	number of objects
DA	2488
DB	408
DAB/DBA	127
DAO	46
DC	214
DZ	44
DQ	57
CV	27
Magnetic WD	60
WD+MS	89
NLHS	902
QSO	3735
Unreliable	16
Unclassified	2
New spectroscopically confirmed WDs	1752

contaminants. As a further test, we also decided to calculate values of completeness and efficiency using only objects with new DR9/10 spectra (Fig. 9) in the same way we did before using the DR7 training sample (Sect. 3). Even though this new spectroscopic sample is considerably smaller than the DR7 training sample, the calculated values of completeness and efficiency are similar; e.g. selecting objects with $P_{WD} \geq 0.41$ achieves a completeness of 96% and an efficiency of 86.4% on the DR9/10 spectroscopic sample, comparable to the completeness of 95% and an efficiency of 89.7% achieved for the training sample.

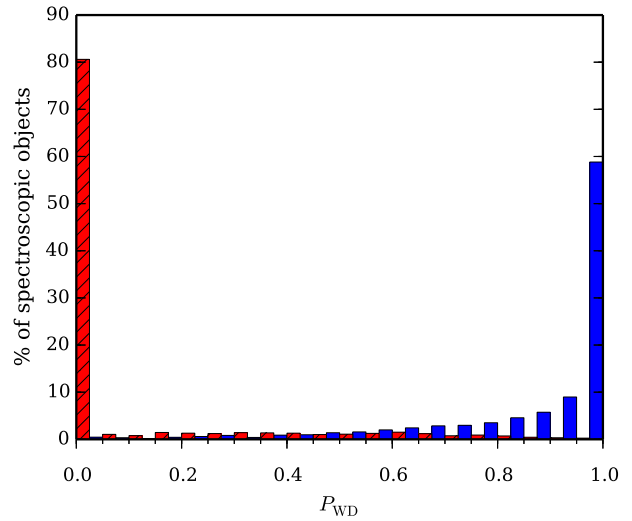


Figure 8. Distribution of 8034 spectroscopically identified white dwarfs (blue) and contaminants (red, shaded) with proper motions from the sample of objects with new DR9/10 spectra

as a function of P_{WD} .

5 A CATALOGUE OF PHOTOMETRIC WHITE DWARFS CANDIDATES IN DR10

We retrieved *ugriz* photometry and proper motions for all the primary point sources in DR10 using the criteria described in Table 2, but adding the additional constraint that the selected objects must have proper motions. Furthermore, having to rely only on photometric data we decided to also exclude objects that were flagged as having too few good detections and saturated pixels. This results in a total of 61969 photometric objects. We calculated RPMs for these objects and, using the probability map created with the DR7 training sample (Sect. 3), we calculated their P_{WD} . Our catalogue can be easily used as the starting point for creating different white dwarf candidates samples according to the compromise between completeness and efficiency best suited for different specific uses. Table 5 illustrate the structure and the content of the catalogue, the full list of objects can be accessed online via the VizieR catalogue access tool.

6 SDSS SPECTROSCOPIC COVERAGE

6.1 SDSS objects with multiple spectra

About 24% of the objects in the spectroscopic samples inspected as part of this work have multiple spectra resulting from repeat observations of plates or overlapping regions between plates. Most of these have 2-4 spectra taken with either SDSS or BOSS, but we also found a few white dwarfs with up to 16 spectra. Concerning the work we describe in this paper, multiple spectra were only inspected for objects with a dubious classification. However, these spectra are a precious resource which can be used to investigate systematic uncertainties in stellar parameter obtained by spectral modelling and to probe for variability of spectral features. For these reasons, in addition to our photometric catalogue of white dwarf candidates, we also provide a list of the avail-

Table 5. Format of the DR10 catalogue of white dwarf candidates. The full catalogue can be accessed online via the VizieR catalogue tool.

Column No.	Heading	Description
1	sdss name	SDSS objects name (SDSS + J2000 coordinates)
2	SDSS-III photoID	Unique ID identifying the photometric source in SDSS-III
3	SDSS-II photoID	Unique ID identifying the photometric source in SDSS-II
4	ra	right ascension (J2000)
5	dec	Declination (J2000)
6	ppmra	proper motion in right ascension (mas/yr)
7	ppmra err	proper motion in right ascension uncertainty (mas/yr)
8	ppmdec	proper motion in right declination (mas/yr)
9	ppmdec err	proper motion in right declination uncertainty (mas/yr)
10	probability	The <i>probability of being a WD</i> computed for this object
11	umag	SDSS <i>u</i> band PSF magnitude
12	umag err	SDSS <i>u</i> band PSF magnitude uncertainty
13	gmag	SDSS <i>g</i> band PSF magnitude
14	gmag err	SDSS <i>g</i> band PSF magnitude uncertainty
15	rmag	SDSS <i>r</i> band PSF magnitude
16	rmag err	SDSS <i>r</i> band PSF magnitude uncertainty
17	imag	SDSS <i>i</i> band PSF magnitude
18	imag err	SDSS <i>i</i> band PSF magnitude uncertainty
19	zmag	SDSS <i>z</i> band PSF magnitude
20	zmag err	SDSS <i>z</i> band PSF magnitude uncertainty
21	instrument	instrument used to take the most recent spectrum of the object (SDSS or BOSS)
22	specobjID SDSS-III	unique ID identifying the spectroscopic source in SDSS-III
23	specobjID SDSS-II	unique ID identifying the spectroscopic source in SDSS-II
24	human class	classification of the object based on our visual inspection of its spectrum
25	Kleinman class	classification of the object according to Kleinman et al. (2013)
26	Kepler class	classification of the object according to Kepler et al. (2015)
27	ancillary flag	1 indicates the object was part of the BOSS WD and subdwarfs ancillary program
28	SDSS WD	1 indicates that the objects was classified as a WD based on available SDSS spectra
29	BOSS WD	1 indicates that the objects was classified as a WD based on available BOSS spectra
30	Brown WD flag	1 indicates that the objects was classified as a WD in the the hypervelocity stars spectroscopic survey (Brown et al. 2006, 2007a, 2007b). 2 indicates that the object was classified as something other than a WD
31	Simbad classification	Currently available Simbad classifications
32	DR7 extension	1 indicates that the objects was included as part of the DR7 extension (Sect. 7.3)

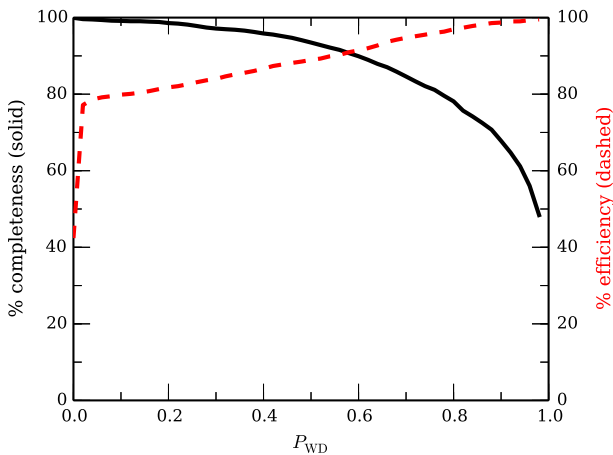


Figure 9. Completeness (solid line) and efficiency (dashed line) of samples of white dwarf candidates from our catalogue shown as functions of the minimum value of P_{WD} an object must have in order to be selected. These values of completeness and efficiency were computed using the SDSS-III spectroscopic sample as a reference.

able spectra (identifiable via *MJD*, *plate ID* and *fiber ID*) for all the objects in our catalogue (including the DR7 extension, sect. 7.3).

6.2 SDSS white dwarf spectroscopic completeness

Using the P_{WD} in our catalogue and correcting for the completeness of the sample (Fig. 5) one can reliably estimate the total number of bright ($g \leq 19$) white dwarfs with $T_{\text{eff}} \gtrsim 7000$ K in the SDSS photometric footprint. The ratio of spectroscopically confirmed white dwarfs to this total number of white dwarfs can be used as an estimate of the spectroscopic completeness of SDSS white dwarfs both in terms of spatial and colour distribution. As mentioned before, most of the SDSS white dwarfs are only serendipitous spectroscopic targets, so it comes with no surprise that the average spectroscopic completeness of SDSS white dwarfs is only $\sim 40\%$. However, this number is averaged over the entire SDSS photometric footprint, large areas of which have not yet received any spectroscopic follow up (Fig. 1). In Fig. 10 we show that over the spectroscopic footprint (which covers most of the northern galactic cap), the average spectroscopic completeness of SDSS white dwarfs is actually closer to $\sim 75\%$.

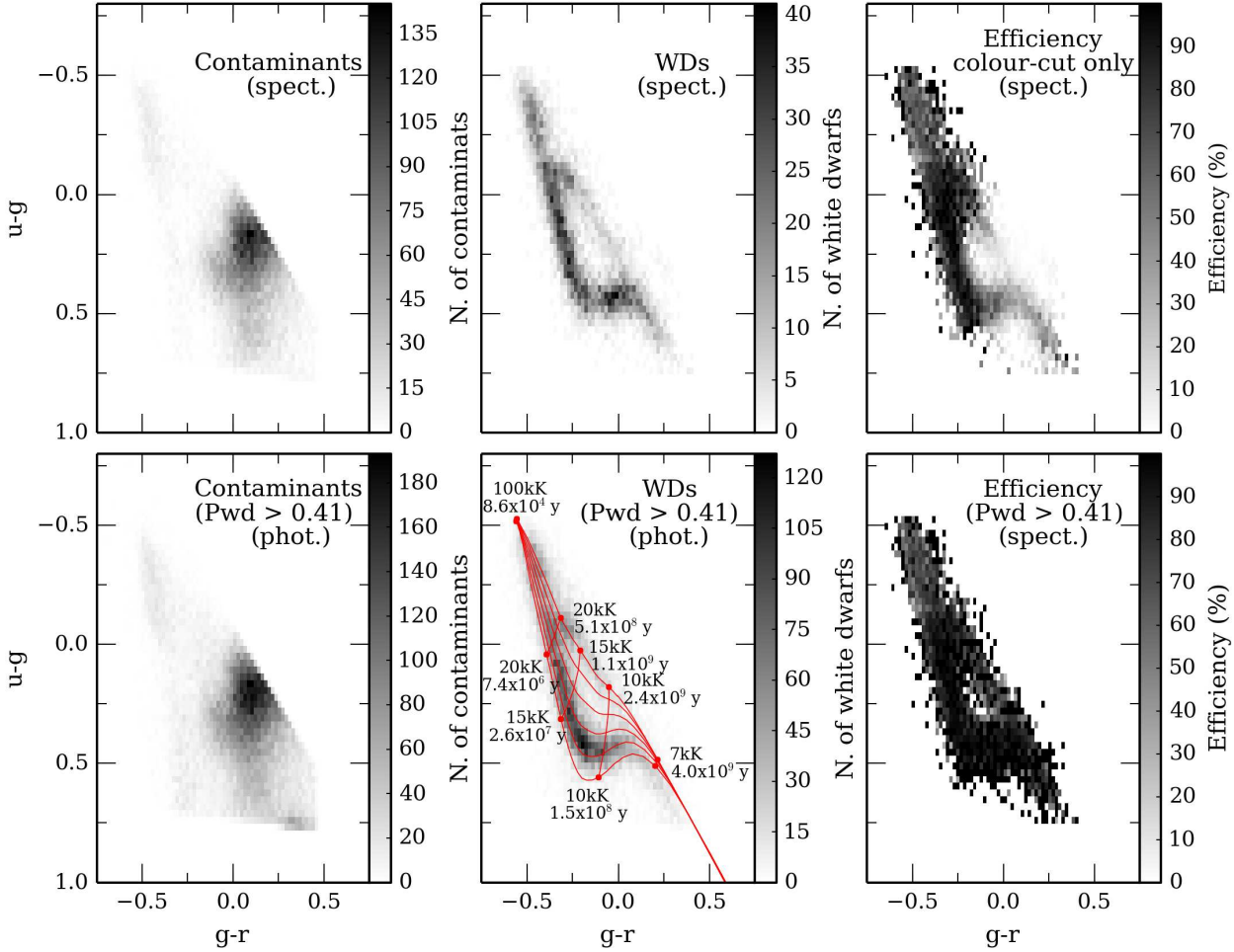


Figure 7. DR7 spectroscopic training sample (27639 objects, top) and DR10 photometric sample (61969 objects, bottom) within our initial $(u - g, g - r)$ colour-colour selection. The top left and top middle panels show, respectively, the distribution of the contaminants and the white dwarfs from our initial DR7 spectroscopic sample. The top right panel shows the ratio of spectroscopically confirmed white dwarfs to the total number of objects with spectra in DR7, $N_{WD}/(N_{WD} + N_{Cont})$. The top right panel clearly illustrates the efficiency of a selection which only uses colour cuts. Such selection leaves areas of strong contamination at the red and the blue ends of the $(u - g, g - r)$ colour region. The bottom left panel shows the distribution of all sources from our DR10 photometric catalogue with $P_{WD} < 0.41$; these objects would be considered contaminants when compiling a 95% complete sample. Similarly, the bottom middle panel shows the distribution of all sources from our DR10 photometric catalogue with $P_{WD} \geq 0.41$, these objects would all be considered high-confidence white dwarf candidates when compiling a 95% complete sample. White dwarf cooling tracks are shown in the red overlay. Both photometric distributions are extremely similar to their spectroscopically determined counterparts (top panels). The bottom right panel shows the ratio of spectroscopically confirmed white dwarfs with $P_{WD} \geq 0.41$ to the total number of objects with spectra in DR7 with $P_{WD} \geq 0.41$. This diagrams effectively shows the efficiency of our selection method. Unlike the top right panel, this probability based selection is practically independent of the location in colour space.

However, as shown in Fig. 11, the spectroscopic completeness is also very colour-dependent. Because quasars have always been one of the main targets of SDSS, the colour region populated by quasars has received more intense spectroscopic follow up. Consequently, the spectroscopic completeness of SDSS white dwarfs is highest for white dwarfs with colours similar to those of quasars and therefore $T_{eff} \lesssim 10000$ K. At this cool end in $(u - g, g - r)$ colour space the spectroscopic completeness can be as high as 85%. On the other hand, the colour space occupied by hotter white dwarfs ($T_{eff} \gtrsim 10000$ K) has received much sparser spectroscopic follow-up, which is reflected by the drop in spectroscopic completeness which varies between

$\sim 20\%$ and $\sim 40\%$. Even though these less complete colour regions have been specifically covered by SDSS's ancillary white dwarf follow-up programs (Dawson et al. 2013), the number of white dwarfs observed by these programs only marginally affects the overall completeness (Sect. 6.3). Fig. 10 and 11 clearly illustrate that the current sample of white dwarfs with Sloan's spectroscopy is inhomogeneous both in sky and colour distribution and extreme care should be taken when using it to compute any statistics. Each BOSS plates covers an area of 1.49 deg radius and has 1000 fibers. However, on average, only ~ 4 white dwarfs were targeted on each BOSS plate, with only 2-3 plates having up to ~ 20 white dwarfs and over 350 plates with no white dwarfs at

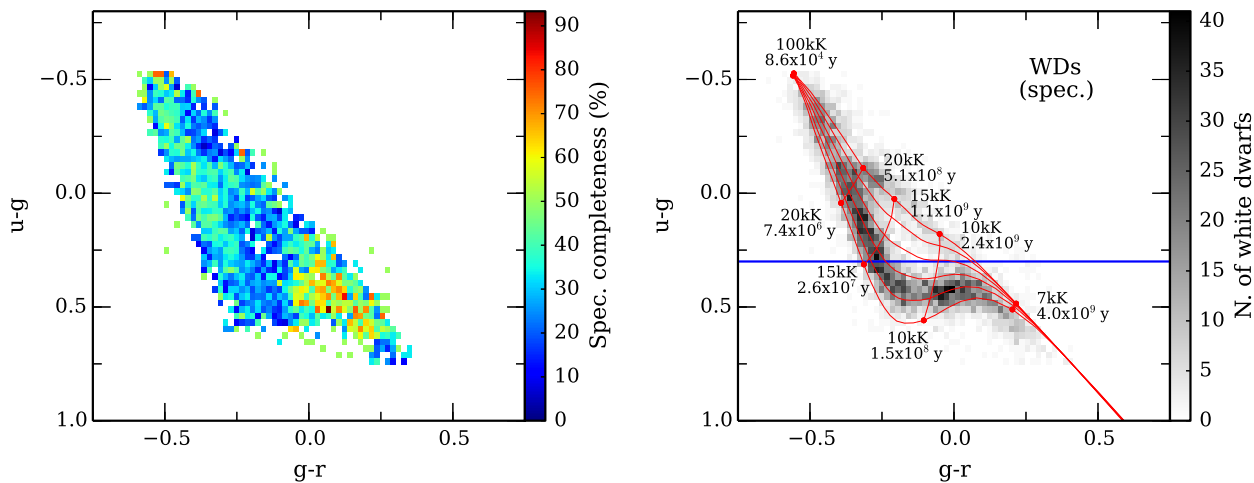


Figure 11. *Left panel:* Spectroscopic completeness of SDSS white dwarfs, computed as the ratio of spectroscopically confirmed white dwarfs to all high-confidence white dwarf candidates ($P_{WD} \geq 0.41$) within our initial ($u-g, g-r$) colour-colour selection.

Right panel: Distribution of spectroscopically confirmed white dwarfs within our initial ($u-g, g-r$) colour-colour selection with cooling tracks shown as overlay. The blue line indicates the $u-g$ cut applied by the SDSS-III white dwarf and hot subdwarf stars ancillary project target selection. Only objects above the blue line were targeted, excluding most of the cool white dwarfs.

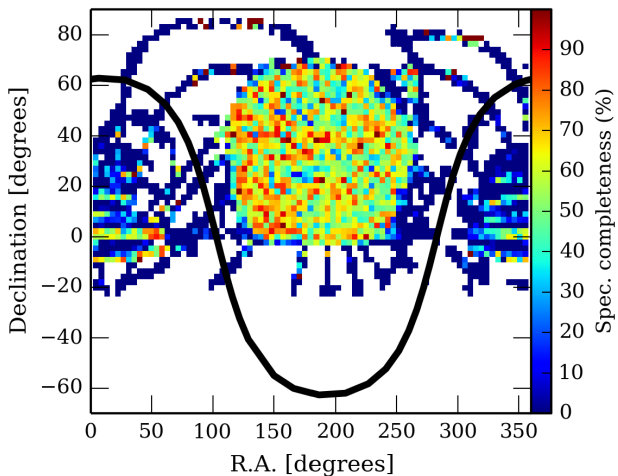


Figure 10. Spectroscopic completeness of SDSS white dwarfs satisfying the criteria in Table 2, computed as the ratio of spectroscopically confirmed white dwarfs to all high-confidence white dwarf candidates ($P_{WD} \geq 0.41$) over the entire photometric footprint of SDSS (Table 5). The black line indicates the location of the galactic plane.

all. Using our photometric catalogue of white dwarf candidates we estimated that on average ~ 13 white dwarfs could have been targeted on each BOSS plate, with some more densely white dwarf-populated plates at low galactic latitudes (Fig. 12). Even these very simple estimates already show that SDSS, or any other similar multi-object spectroscopic survey (i.e. LAMOST Zhao et al. 2013, Zhang et al. 2013; WEAVE (Dalton et al. 2014); 4MOST de Jong et al. 2014), could easily provide spectroscopic follow-up of almost all bright white dwarf candidates with very little expenditure of fibers. In fact, a BOSS-like survey could produce a $> 95\%$ complete, magnitude limited ($g \leq 19$), spectroscopic

sample of white dwarfs by dedicating just over 1% of its fibers to white dwarf follow up. With such a complete and well defined spectroscopic sample it would be possible to carry out extremely reliable and diverse statistical analyses and finally answer many of the open questions about the formation and evolution of white dwarfs and their progenitors. Furthermore such a large spectroscopic sample would include many rare types of white dwarfs.

6.3 SDSS-III white dwarf and hot subdwarf stars ancillary project

About 3.5% of the BOSS fibers in DR9 and DR10 were devoted to 25 small ancillary programs. One of these ancillary programs, the SDSS-III white dwarf and hot subdwarf stars ancillary project, specifically targeted 5709 white dwarf and hot subdwarf candidates selected using colour and proper motion as summarized in Table 6 (Dawson et al. 2013, Ahn et al. 2014). Using the corresponding ancillary target flag (Dawson et al. 2013) we retrieved spectra, $ugriz$ photometry and proper motions of all the targets of this ancillary program. 4104 of these SDSS ancillary targets match the criteria (in either DR7 or DR10) in Table 2 and have proper motions and, therefore, must have been visually classified by us in either the DR7 training sample or the DR9/10 spectroscopic sample. When comparing our classification to the targeting selection of the ancillary project we established that 78% of the ancillary project targets included in our catalogue were classified as white dwarfs by us (Table 7), with the vast majority of the rest being subdwarfs (e.g. Reindl et al. 2014). This comparison shows that the targeting strategy adopted in this ancillary program was very efficient, however the criteria in Table 6 limit the selection to white dwarfs with hydrogen dominated atmospheres (DA) hotter than ~ 14000 K and white dwarfs with helium dominated atmospheres (DB) hotter than ~ 8000 K (Table 6). In conclusion the SDSS-III white dwarf and hot

Table 6. Constraints used to select the targets of the SDSS-III white dwarf and hot subdwarf stars ancillary project (Dawson et al. 2013).

Only areas of DR7 footprint with galactic extinction in r	<	0.5 mag
Colour	constraint	
$(u - g)$	<	0.3
$(g - r)$	<	0.5
$(g - r)$	>	-1
$(u - r)$	<	0.4
g	<	19.2
For objects with		
$(g - r)$	>	-0.1
$(u - r)$	>	-0.1
proper motion	>	20 mas/yr

Table 7. Results of the comparison of the SDSS-III white dwarf and hot subdwarf stars ancillary project with our classification of SDSS spectra.

After inspecting the spectra of the 904 ancillary targets not classified as white dwarfs by us, we are confident that these are most likely hot subdwarfs.

Total number of WDs from the ancillary program included in our catalogue including DR7 extension	4104
Number of ancillary program targets not classified as WDs.	904

subdwarf stars ancillary project significantly contributed in increasing the number of SDSS white dwarfs with spectra, but this sample of white dwarfs produced suffers from various biases and should be handled with extreme care when used for statistical analysis.

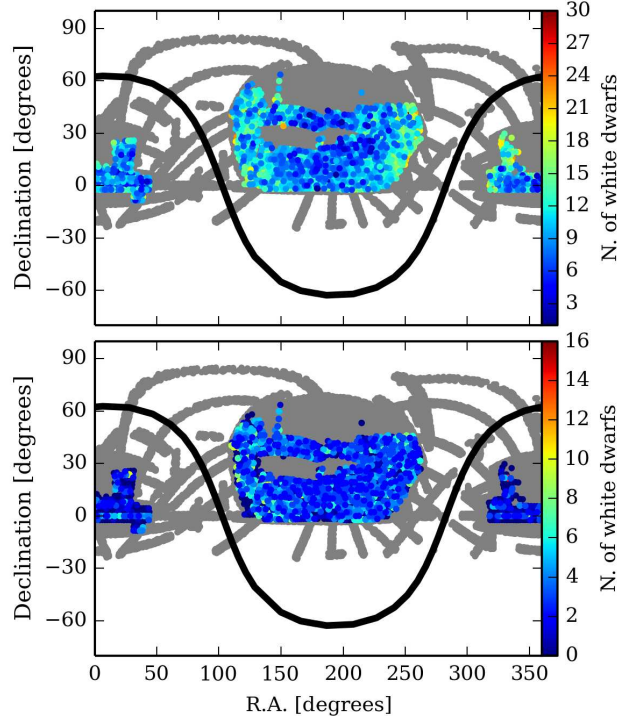
7 LIMITATIONS AND CORRECTIONS

7.1 Proper motions

One of the main limitation of the selection method used to generate this catalogue is that our P_{WD} can only be calculated for objects with proper motions. 3.8% of all the spectroscopically confirmed white dwarfs we examined do not have proper motion and we can therefore expect that our DR10 photometric catalogue is incomplete by ~ 870 white dwarfs candidates on account of them not having proper motion.

7.2 Extremely Low Mass white dwarfs (ELM white dwarfs)

Even though our spectroscopic training sample, initially drawn from a broad colour selection (Fig. 2), includes the vast majority of single white dwarfs (see Sect.8) it does not include some rarer types of white dwarfs with more exotic colours. Extremely low mass (ELM) white dwarfs are likely to be among such rare types (Brown et al. 2010). We tested

**Figure 12.** Location of BOSS plates overlaid on the DR10 photometric footprint (grey). The black line indicates the location of the galactic plane.

Top panel: The colour of the plates indicates the number of high confidence white dwarf candidates ($g \leq 19$) from our catalogue per plate.

Bottom panel: The colour of the plates indicates the number of spectroscopically confirmed bright ($g \leq 19$) white dwarfs which were observed on the BOSS plate and released in DR9/10.

Both panels clearly illustrate that the number of white dwarfs (or white dwarf candidates) per plate decreases with increasing distance from the galactic plane

the ability of our selection method to correctly identify ELM white dwarfs by retrieving the SDSS photometry of all bright ($g \leq 19$) ELM white dwarfs from Gianninas et al. (2014) and verifying whether or not they were recovered in our catalogue. We determined that only 17 out of 37 are included in our catalogue. One of the ELM white dwarfs was excluded because of bad photometry in SDSS, but the remaining 19 were simply outside our initial colour cut. Furthermore ELM white dwarfs have peculiar spectra which can make it hard to correctly classify them as white dwarfs. Of the 17 ELM white dwarfs in our catalogue 11 have either SDSS or BOSS spectra and were therefore visually classified by us. Only one of these ELM white dwarfs was erroneously classified as a NLHS. Consequently we believe that misclassification of ELM white dwarfs in our training sample does not significantly affect our selection method. In fact only 2 of the ELM white dwarfs in our catalogue have $P_{WD} < 0.41$ while the remaining 16 have $P_{WD} > 0.6$. We conclude that ELM white dwarfs within our colour regions would most likely be identified as high confidence white dwarfs candidates.

Table 8. Detailed break down of the reasons why 135 white dwarfs from our DR7 training sample do not figure in the main DR10 photometric catalogue.

29 objects marked as "colours changed" experienced changes in their recorded *ugriz* magnitudes such that in DR10 they would not fall into our initial colour cut.

23 objects marked as "Not in SDSS-III database" either fall in the SEGUE-1 imaging scans which were not included in SDSS-III or are in areas of the sky where, probably because of the new SDSS-III sky subtraction, faint sources near a bright source were not identified (Ahn et al. 2012).

N. of WDs "missing"	Cause
17	<i>type</i> \neq 6 in DR10
63	<i>gmag</i> > 19 in DR10
29	colours changed
3	No recorded proper motion in DR10
23	Not in SDSS-III database
135	

7.3 DR7 to DR10 miss-matches: the "DR7 extension"

When trying to retrieve the 6706 white dwarfs with proper motions of our DR7 spectroscopic training sample (Sect. 2) from our DR10 photometric catalogue, we noticed that some DR7 objects could not be correctly matched in DR10. The cross matching of DR7 spectra to DR10 photometric sources was done using modified Julian date (MJD), plate ID and fiber ID which, together, uniquely identify any spectrum in SDSS. This was faster and more reliable than a coordinate cross match using the entire DR10 photometric database or a specifically selected subset of it (some objects underwent changes in coordinates, photometry or flags in between data releases). Furthermore, in this way, we were able to check that the DR7 spectra were still available in DR10 and to check for other possible incongruences between the data releases. To our surprise we found that our DR10 photometric sample only included 6560 of the spectroscopically confirmed white dwarfs. We determined that 11 of the "missing objects" could not be matched to sources in DR10 because the MJD with which their spectra were identified changed between DR7 and DR10¹. However the objects are included in the DR10 photometric sample and therefore the cross-match was manually corrected and our count was updated to 6571 retrieved DR7 white dwarfs. The remaining 135 white dwarfs are missing from the photometric DR10 sample because of differences in their photometry or flags in DR10 compared to DR7 (Table 8).

In order to make our catalogue as complete as possible we decided to add a "DR7 extension" to our original list of 61969 DR10 white dwarf candidates. This extension was created by recovering *ugriz* photometry for all reliable primary photometric sources in DR7 that satisfied the criteria described in Table 2 and then selecting only those objects that did not appear among the 61969 DR10 photometric candidates. The cross-matching between DR9/DR10 and DR7

¹ From the spectra we examined, we determined that MJDs uniquely identifying SDSS spectra have changed between DR7 and 10 for the following plates: 0389, 2129, 2516, 2713, 2865.

Table 9. Classification of the 297 objects with BOSS spectra, found in our "DR7 extension". 29 of the new spectroscopically confirmed white dwarfs had not received spectroscopic follow-up before DR9.

Class	number of objects
DA	32
DB	7
DAB/DBA	1
DAO	0
DC	4
DZ	0
DQ	1
Magnetic WD	0
WD+MS	6
CV	2
NLHS	21
QSO	222
Unreliable	1
Unclassified	0
New spectroscopically confirmed WDs	29

photometric sources was done by comparing sky coordinates using a 1 arcsecond matching radius which generated a list of 3799 DR7 objects. 689 of these do not have any counterpart in DR10 as they either fall in the SEGUE-1 imaging scans which were not included in SDSS-III or are in areas of the sky where, probably because of the new SDSS-III sky subtraction, faint sources near a bright source were not extracted (Ahn et al. 2012). The remaining 3110 are objects whose photometric data or flags have changed between data releases such that they no longer fulfil the criteria in Table 2 in DR9/10. As a final check we confirmed that the "DR7 extension" includes all of the 135 white dwarfs that were spectroscopically identified in DR7, but which were missing in our DR10 photometric catalogue (Table 8). Furthermore within the "DR7 extension" we were also able to identify and classify 29 new white dwarfs which only have BOSS spectroscopy (Table 9).

7.4 DR10 to DR7 miss-matches

In the previous paragraph we discussed how a few objects which fulfilled our selection criteria (Table. 2) in DR7 did not do so in DR10. Similarly we expected to find some sources with DR7 spectra which did not fulfil our selection criteria in DR7 but do so in DR10 and therefore would be included in our main photometric sample. From our 61969 photometric candidates we selected all objects with SDSS-II spectroscopy which were not included in our initial DR7 spectroscopic sample, and therefore already classified. We identified 2071 of these SDSS-II spectroscopic sources which we had not yet inspected even though they were included in our catalogue.

Once again the main reasons for the "appearance" of these sources in our DR10 selection are: changes in their *g* magnitude which may have moved an object below our $g \leq 19$ limit; corrections of flags of objects previously, erroneously, classified as "extended sources" and inclusion of proper motions for objects which did not previously have

Table 10. Classification of the 2071 objects with SDSS spectra which did not fulfil our selection criteria in DR7 but did so in DR10

Class	number of objects
CV	6
DA	136
DB	12
DAB	27
DAO	1
DC	14
DZ	3
DQ	5
Magnetic WD	1
WD+MS	9
NLHS	95
QSO	1675
Unclassified	2
unreliable	84

one. However, we also identified 31 sources in our DR10 sample with SDSS spectra which simply do not have any DR7 photometry (in our catalogue they lack a DR7 photometric ID). In order to keep our catalogue as consistent and complete as possible, we decided to retrieve spectra for these 2071 sources (using the DR7 photometric ID included in our table) and proceeded to visually classify them. The results of the classification of these 2071 objects are shown in Table 10.

8 COMPARISON WITH OTHER CATALOGUES

8.1 Kleinman et al 2013

The Kleinman et al. (2013) catalogue of spectroscopically identified DR7 white dwarfs contains 20407 spectra corresponding to 19712 unique objects of which only 7424 are brighter than $g=19$. Unlike our spectroscopic samples (DR7 training sample and DR9/DR10 BOSS sample) the Kleinman et al. (2013) catalogue does not have a set magnitude limit and includes spectra of extremely faint objects. Most of these have low signal to noise ratios making the classification, for at least some of them, inevitably less reliable. In order to carry out a comparison between our spectral classification and Kleinman’s we proceeded to cross match the Kleinman et al. (2013) catalogue of DR7 white dwarfs with the DR10 *specphotoall* table using modified Julian date (MJD), plate ID and fiber ID and obtained SDSS-III IDs for these objects. Analogously to what is described in section 6.2, 52 spectra could initially not be matched to DR10 sources because of changes in the MJD and another 149 spectra could not be matched because the corresponding photometric sources are not included in the DR10 photometric database. 861 more white dwarfs were rejected by our selection because of their colour, flags or lack of recorded proper motion (Table A1). After manually correcting the miss-matching MJDs and including the “DR7 extension” discussed before, we established that our catalogue includes 6689 objects classified as white dwarfs by Kleinman et al. (2013).

Table 11. Detailed break down of the reasons why 861 white dwarfs from the Kleinman et al. (2013) catalogue are not included in our main DR10 photometric catalogue. Most of these are white dwarfs with a main sequence companion. Note that 119 of these were recovered in our “DR7 extension” (sect 7.3)

Keinman WDs excluded in DR10 photometric catalogue	Cause
601	Excluded by criteria in Table 2
260	No proper motion
861	

Inspecting the results of our spectroscopic classification, we find that we also identified 99.6% of these 6689 objects as white dwarfs. Only 30 (0.4%) of Kleinman’s white dwarfs were classified as contaminants by us when preparing the spectroscopic training sample (Sect. 3). We closely re-examined all available spectra for these 30 objects. We confirm our initial classification of 20 objects as contaminants (18 NLHS and 2 QSO), and one object as “unclassified” because of the very low quality of its spectrum. However we concede that the remaining 9 objects are most likely white dwarfs and our initial classification was wrong.

Our catalogue also includes 261 objects with DR7 spectroscopy which we classified as white dwarfs, but which are not included in Kleinman et al. (2013) (Table 1). Kleinman et al. (2013) do *not* include a list of all spectra that they processed, and we have therefore no way to assess whether they inspected those objects. We conclude that our classification is remarkably close to Kleinman’s and the disagreement over a very limited number of objects in our training sample does not effect our selection method.

Furthermore, unlike Kleinman et al. (2013), we aim to provide a well defined sample SDSS white dwarfs candidates without being limited by the availability of spectroscopy. Our catalogue contains ~ 23000 high-confidence bright ($g \leq 19$) white dwarfs candidates, over 3 times the number of white dwarfs in Kleinman et al. (2013) catalogue with the same magnitude limit, underlining the remaining potential for follow up spectroscopy.

8.2 Hypervelocity stars. I,II,III (Brown et al 2006, 2007a, 2007b)

The hypervelocity stars spectroscopic survey (Brown et al. 2006, 2007a, 2007b) identified a total of 260 white dwarfs serendipitously found among B star candidates. 48 of these white dwarfs have $g > 19$ and are therefore not included in our photometric sample; another 9 are excluded by our initial selection criteria (Table 2) and 23 more do not have proper motions in SDSS DR9/10. This leaves 180 white dwarfs spectroscopically identified by Brown et al. which are included in our DR10 photometric catalogue and which we flag as “known white dwarfs”. Our catalogue also includes 296 hypervelocity survey targets which were classified as “non white dwarfs” by Brown et al. We flagged these objects to recognise them as “known contaminants”. Even though this sample of confirmed white dwarfs and contaminants is quite small, it was selected and classified completely

independently from our work. Therefore these white dwarfs and contaminants are valuable test objects to verify once more the reliability of our P_{WD} .

We established that the vast majority of the 180 white dwarfs have P_{WD} greater than 0.9 and only 11 of them have probabilities lower than 0.6. Out of the 296 contaminants 34 have P_{WD} greater than 0.5, however only 11 of them have probability values higher than 0.7. In conclusion our P_{WD} seems to be somewhat weaker when trying to separate these contaminants as they were specifically selected as objects with colours similar to those of typical white dwarf *and* to have high proper motions.

8.3 Follow-up spectroscopy: 11 new white dwarfs

As a final test for our selection method we selected 17 white dwarfs candidates from our catalogue which did not have a SDSS or BOSS spectrum (at the time of DR9) and spanned a wide range of P_{WD} . On June 7th and 8th 2013, we obtained spectroscopy of these 17 objects using the double-armed Intermediate Resolution Spectrograph² (ISIS) on the William Herschel Telescope (WHT) on the island of La Palma. We observed under 1" seeing conditions. We used the R600R and R600B gratings in the ISIS blue and red arms respectively, with a 1" slit. The blue arm was centred at 4351Å and the red arm at 6562Å. The blue spectra covered a total wavelength range from ~3700Å to ~5000Å and the red spectra ranged from ~5700Å to ~7200Å. The spectral resolution is ~2 Å and ~1.8 Å in the red and in the blue arm respectively. Two consecutive 10 minute exposures were taken in order to increase the signal-to-noise ratio (S/N) of the average spectrum. We adopted a standard reduction and calibration for the spectra (Greiss et al. 2014). The spectra allowed us to classify our candidates and corroborate the validity of our P_{WD} : the 9 targets with $P_{WD} \geq 0.89$ were all confirmed as white dwarfs, out of 4 intermediate probability candidates ($> 0.45, < 0.7$) only the highest probability candidate was confirmed as a white dwarf and finally only one of the 4 low probability targets (< 0.39) is a white dwarf (Table 12, Fig.13, Fig.14). The release of DR10 added new BOSS spectra, compared to DR9, and 3 of the photometric candidates we spectroscopically followed-up now also have BOSS spectra (SDSSJ1354+2530, SDSSJ1439+2344, SDSSJ1306+1333; marked with * in Table.12). Visual inspection of these BOSS spectra confirmed our classification based on the ISIS spectra.

9 CONCLUSION

We developed a selection method for white dwarfs which allows to reliably select white dwarf candidates relying on their colours and reduced proper motion. By using the distribution of a large sample of spectroscopically confirmed white dwarfs and contaminants in colour-RPM space we calculate a *probability of being a WD* (P_{WD}) for any object with available multi-band photometry and proper motion. The spectroscopic sample used to develop our selection method was created by classifying over 27000 spectra of blue

objects from SDSS DR7. In developing our selection method we decided limit our efforts to bright objects ($g \leq 19$) as fainter sources are less likely to have reliable detections on the historic photographic plates, necessary to calculate proper motions. We used our selection method to calculate P_{WD} for 61969 primary photometric point sources selected from SDSS DR10 and for 3799 primary point sources selected from SDSS DR7 which fulfilled our selection criteria in DR7, but have incomplete data in the following DRs. This catalogue of over 65000 objects with calculated P_{WD} contains 8699 objects with available Sloan spectroscopy which we classified as white dwarfs. Using different values of P_{WD} as threshold, one can produce white dwarf candidates samples based on the compromise between completeness and efficiency best suited for different specific uses. Even though we developed our method using SDSS DR7 and here we present its application to SDSS DR10, it can be used on any sample of objects having multi band photometry and proper motions. We estimate that our SDSS DR10 photometric catalogue contains ~ 23000 high confidence white dwarf candidates of which ~ 14000 have not been followed up spectroscopically. These statistics imply that the spectroscopic sample of SDSS white dwarfs is currently, on average, only ~ 40% complete for white dwarfs with $T_{\text{eff}} \gtrsim 7000$ K and $g \leq 19$, underlining the remaining potential for follow-up spectroscopy.

10 ACKNOWLEDGEMENTS

NPGF acknowledge the support of Science and Technology Facilities Council (STFC) studentships.

The research leading to these results has received funding from the European Research Council under the European Union's Seventh Framework Programme (FP/2007-2013) / ERC Grant Agreement n. 320964 (WDTracer).

Funding for SDSS-III has been provided by the Alfred P. Sloan Foundation, the Participating Institutions, the National Science Foundation, and the U.S. Department of Energy Office of Science. The SDSS-III web site is <http://www.sdss3.org/>. We thank S.O. Kepler for a constructive referee report and Daniel Eisenstein for comments on the originally submitted manuscript. The William Herschel Telescope is operated on the island of La Palma by the Isaac Newton Group in the Spanish Observatorio del Roque de los Muchachos of the Instituto de Astrofísica de Canarias.

APPENDIX A: COMPARISON WITH KEPLER ET AL. 2015

After submission of this paper, Kepler et al. (2015) posted a catalogue of 9088 white dwarfs and subdwarfs spectroscopically identified among the SDSS spectra obtained after DR7. For completeness, we compare our classification of objects with new DR9/10 spectra (Sect. 4) with Kepler's catalogue. Our catalogue includes 2041 white dwarfs and 590 subdwarfs from the Kepler et al. (2015) catalogue. Inspecting the results of our spectroscopic classification, we find that of these 2041 objects classified as white dwarfs by Kepler, 88.5% were also identified as white dwarfs by us. 234 (11.5%) of Kepler's white dwarfs were, instead, classified as contaminants

² <http://www.ing.iac.es/Astronomy/instruments/isis/>

Table 12. Results of classification of the newly acquired ISIS spectra for 17 white dwarfs candidates from our catalogue. In the case of DA white dwarfs we also include effective temperature and surface gravity calculated by fitting the spectra with 1-D atmospheric models.

SDSS name	probability of being a WD	classification	T_{eff} (K)	log g
SDSSJ141455.36+240839.0	1.000	DA	15071 ± 72	7.560 ± 0.018
SDSSJ134231.80+043517.4	0.999	DA	20566 ± 65	7.770 ± 0.019
SDSSJ135024.28+052252.3	0.999	DA	22037 ± 94	8.010 ± 0.020
SDSSJ143953.64+234453.6*	0.993	DA	24726 ± 9	8.080 ± 0.010
SDSSJ160726.61+532246.7	0.991	DA	12976 ± 98	8.010 ± 0.030
SDSSJ131825.92+500351.7	0.985	DC	-	-
SDSSJ154621.86+560325.8	0.941	DA	15422 ± 103	7.950 ± 0.017
SDSSJ135451.45+253048.0*	0.933	DA	28389 ± 54	7.960 ± 0.024
SDSSJ132936.48+532211.3	0.891	DA	17707 ± 68	7.860 ± 0.016
SDSSJ134614.32+080411.2	0.696	DA	16525 ± 91	8.260 ± 0.022
SDSSJ145042.93+094055.9	0.566	NLHS	-	-
SDSSJ121910.44+230020.7	0.523	NLHS	-	-
SDSSJ144601.03+483057.7	0.455	NLHS	-	-
SDSSJ130625.92+133349.2*	0.355	NLHS	-	-
SDSSJ154843.29+472936.2	0.315	DB	-	-
SDSSJ143554.16+544448.2	0.288	NLHS	-	-
SDSSJ134700.48+111123.8	0.250	NLHS	-	-

Table A1. Result of the comparison between our classification of objects with spectra taken after DR7 and Kepler et al. (2015) catalogue.

WDs from Kepler et al. (2015) included in our catalogue	2041
subdwarfs from Kepler et al. (2015) included in our catalogue	590
Kepler et al. (2015) WDs not classified as WDs by us	234
Kepler et al. (2015) subdwarfs classified as WDs by us	5
Objects with a DR9/10 spectrum classified by us as WDs, not included in the Kepler et al. (2015) catalogue	57

by us (Sect. 4). We closely re-examined all available spectra for these 234 objects, and confirm our classification of NLHS for 223 objects, but concede that the remaining 11 are likely white dwarfs. From this comparison with Kepler et al. (2015) and also by inspecting Werner et al. (2014), we conclude that most of the white dwarfs that we erroneously classified as NLHS are DAO, PG1159 and O(He) (pre-) white dwarfs. Given that these are rare objects, their erroneous classification does not affect the statistical properties of our selection method and white dwarf candidate sample”.

Our catalogue also includes 57 objects with DR9/10 spectroscopy which we classified as white dwarfs, but which are not included in Kepler’s list (Table A1). Kepler do not include a list of all spectra that they processed, and we have therefore no way to assess whether they inspected those objects.

REFERENCES

- Abazajian, K. N., et al., 2009, *ApJS*, 182, 543
Ahn, C. P., et al., 2012, *ApJS*, 203, 21
Ahn, C. P., et al., 2014, *ApJS*, 211, 17
Bergeron, P., Saffer, R. A., Liebert, J., 1992, *ApJ*, 394, 228
Brown, W. R., Geller, M. J., Kenyon, S. J., Kurtz, M. J., 2006, *ApJ*, 647, 303
Brown, W. R., Geller, M. J., Kenyon, S. J., Kurtz, M. J., Bromley, B. C., 2007a, *ApJ*, 660, 311
Brown, W. R., Geller, M. J., Kenyon, S. J., Kurtz, M. J., Bromley, B. C., 2007b, *ApJ*, 671, 1708
Brown, W. R., Kilic, M., Allende Prieto, C., Kenyon, S. J., 2010, *ApJ*, 723, 1072
Brown, W. R., Kilic, M., Allende Prieto, C., Kenyon, S. J., 2012, *ApJ*, 744, 142
Castanheira, B. G., et al., 2004, *A&A*, 413, 623
Cojocaru, R., Torres, S., Isern, J., García-Berro, E., 2014, 566, A81
Dalton, G., et al., 2014, in *Society of Photo-Optical Instrumentation Engineers (SPIE) Conference Series*, vol. 9147 of *Society of Photo-Optical Instrumentation Engineers (SPIE) Conference Series*, p. 0
Dawson, K. S., et al., 2013, *AJ*, 145, 10
De Gennaro, S., von Hippel, T., Winget, D. E., Kepler, S. O., Nitta, A., Koester, D., Althaus, L., 2008, *AJ*, 135, 1
de Jong, R. S., et al., 2014, in *Society of Photo-Optical Instrumentation Engineers (SPIE) Conference Series*, vol. 9147 of *Society of Photo-Optical Instrumentation Engineers (SPIE) Conference Series*, p. 0
Debes, J. H., Hoard, D. W., Wachter, S., Leisawitz, D. T., Cohen, M., 2011, 197, 38
Doherty, C. L., Gil-Pons, P., Siess, L., Lattanzio, J. C., Lau, H. H. B., 2015, 446, 2599
Dufour, P., Kilic, M., Fontaine, G., Bergeron, P., Lachapelle, F., Kleinman, S. J., Leggett, S. K., 2010, *ApJ*, 719, 803
Dufour, P., et al., 2007, *ApJ*, 663, 1291
Eisenstein, D. J., et al., 2006, *ApJS*, 167, 40
Falcon, R. E., Winget, D. E., Montgomery, M. H., Williams, K. A., 2010, *ApJ*, 712, 585
Farihi, J., Becklin, E. E., Zuckerman, B., 2005, *ApJS*, 161, 394
Farihi, J., Jura, M., Zuckerman, B., 2009, *ApJ*, 694, 805
Gänsicke, B. T., Euchner, F., Jordan, S., 2002, *A&A*, 394, 957

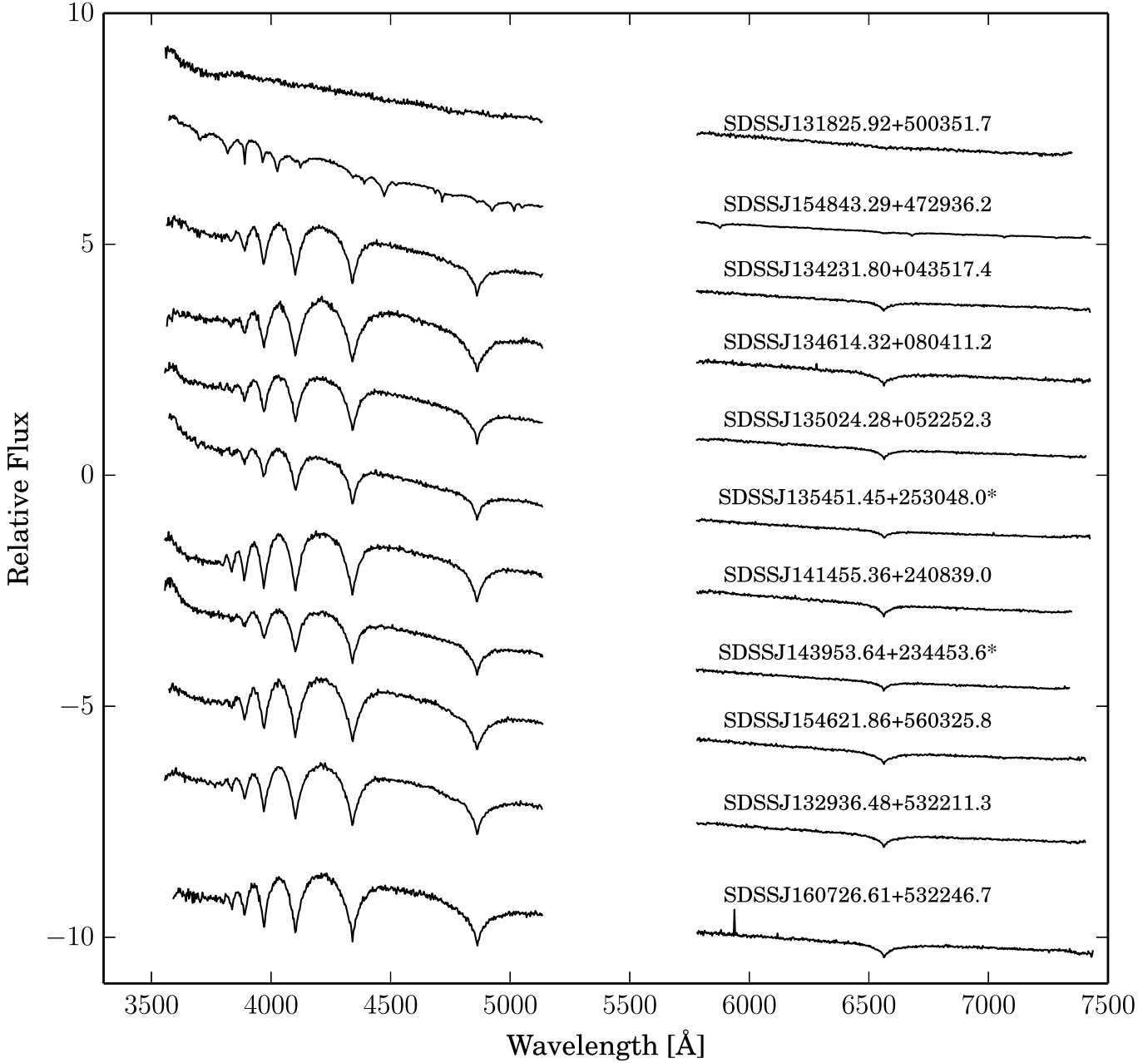


Figure 13. WHT ISIS spectra (blue arm + red arm; R600 grating) of the 11 white dwarf candidates which were confirmed as white dwarfs. Each spectrum is labelled with the SDSS name. Objects marked with * have a new BOSS spectrum released in DR10

Gänsicke, B. T., Marsh, T. R., Southworth, J., Rebassa-Mansergas, A., 2006, *Science*, 314, 1908
Gänsicke, B. T., Koester, D., Girven, J., Marsh, T. R., Steeghs, D., 2010, *Science*, 327, 188
Giammichele, N., Bergeron, P., Dufour, P., 2012, 199, 29
Gianninas, A., Dufour, P., Kilic, M., Brown, W. R., Bergeron, P., Hermes, J. J., 2014, *ApJ*, 794, 35
Girven, J., Gänsicke, B. T., Steeghs, D., Koester, D., 2011, *MNRAS*, 417, 1210
Greiss, S., Gänsicke, B. T., Hermes, J. J., Steeghs, D., Koester, D., Ramsay, G., Barclay, T., Townsley, D. M., 2014, 438, 3086
Harris, H. C., et al., 2003, *AJ*, 126, 1023

Hermes, J. J., et al., 2014, 792, 39
Holberg, J. B., Oswalt, T. D., Sion, E. M., 2002, *ApJ*, 571, 512
Holberg, J. B., Sion, E. M., Oswalt, T., McCook, G. P., Foran, S., Subasavage, J. P., 2008, *AJ*, 135, 1225
Iben, I. J., Ritossa, C., Garcia-Berro, E., 1997, *ApJ*, 489, 772
Kepler, S. O., Kleinman, S. J., Nitta, A., Koester, D., Castanheira, B. G., Giovannini, O., Costa, A. F. M., Althaus, L., 2007, *MNRAS*, 375, 1315
Kepler, S. O., et al., 2013, 429, 2934
Kepler, S. O., et al., 2015, 446, 4078
Kleinman, S. J., et al., 2013, *ApJS*, 204, 5

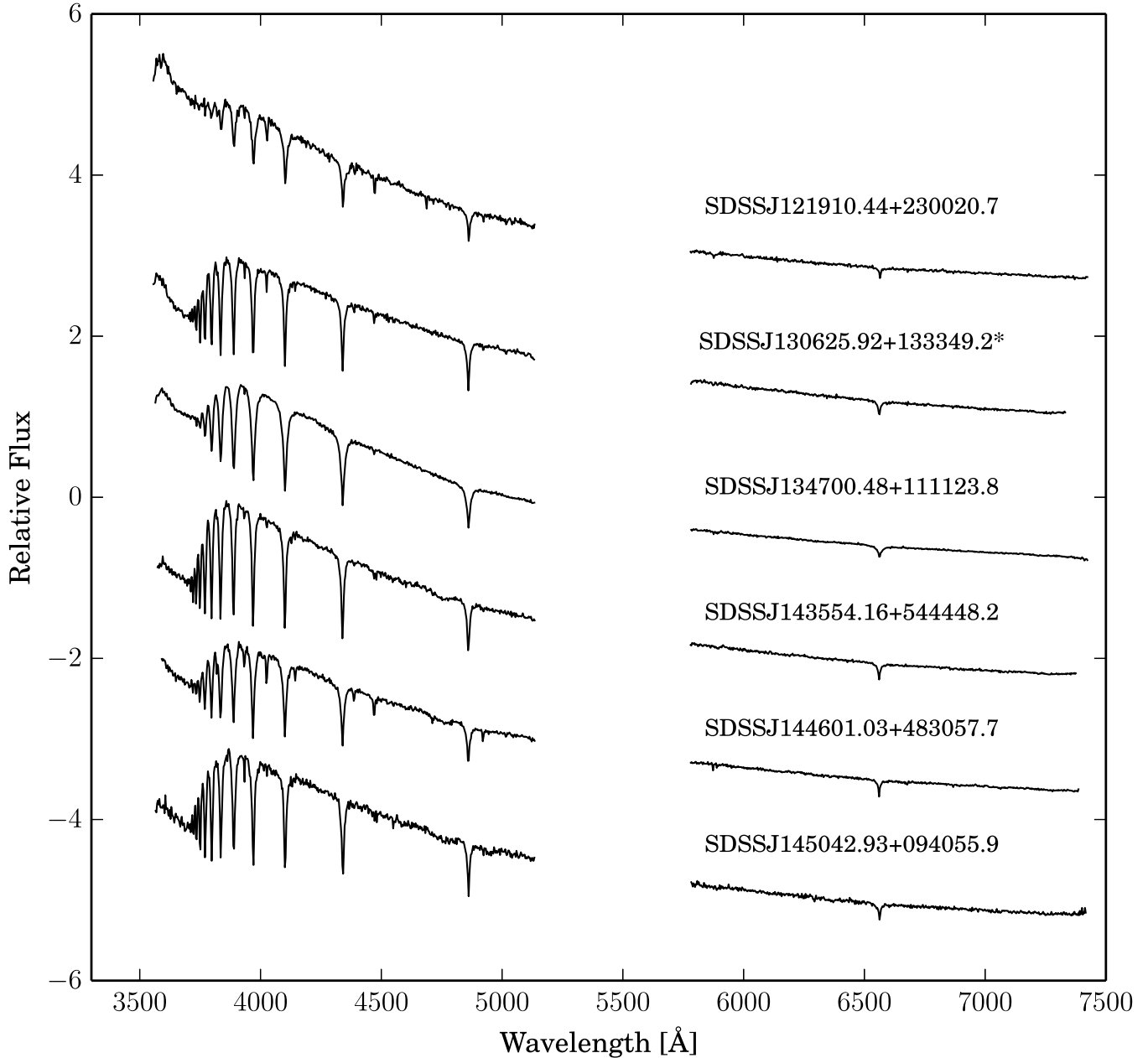


Figure 14. WHT ISIS spectra (blue arm + red arm; R600 grating) of the 6 white dwarf candidates which were later classified as NLHS. Each spectrum is labelled with the SDSS name. Objects marked with * have a new BOSS spectrum released in DR10

Koester, D., Gänsicke, B. T., Farihi, J., 2014, *A&A*, 566, A34
 Külebi, B., Jordan, S., Euchner, F., Gänsicke, B. T., Hirsch, H., 2009, *A&A*, 506, 1341
 Liebert, J., Bergeron, P., Holberg, J. B., 2005, *ApJS*, 156, 47
 Limoges, M.-M., Lépine, S., Bergeron, P., 2013, *AJ*, 145, 136
 Marsh, T. R., Nelemans, G., Steeghs, D., 2004, 350, 113
 Oswalt, T. D., Smith, J. A., Wood, M. A., Hintzen, P., 1996, *Nat*, 382, 692
 Parsons, S. G., Marsh, T. R., Gänsicke, B. T., Drake, A. J.,

Koester, D., 2011, 735, L30
 Reindl, N., Rauch, T., Werner, K., Kepler, S. O., Gänsicke, B. T., Gentile Fusillo, N. P., 2014, 572, A117
 Sayres, C., Subasavage, J. P., Bergeron, P., Dufour, P., Davenport, J. R. A., AlSaiyad, Y., Tofflemire, B. M., 2012, 143, 103
 Schmidt, G. D., Liebert, J., Harris, H. C., Dahn, C. C., Leggett, S. K., 1999, *ApJ*, 512, 916
 Schmidt, G. D., et al., 2003, *ApJ*, 595, 1101
 Sion, E. M., Leckenby, H. J., Szkody, P., 1990, *ApJ Lett.*, 364, L41
 Sion, E. M., Holberg, J. B., Oswalt, T. D., McCook, G. P.,

- Wasatonic, R., Myszka, J., 2014, 147, 129
Smartt, S. J., Eldridge, J. J., Crockett, R. M., Maund, J. R., 2009, MNRAS, 395, 1409
Steele, P. R., et al., 2013, 429, 3492
Tremblay, P.-E., Ludwig, H.-G., Steffen, M., Freytag, B., 2013, 559, A104
Vennes, S., Kawka, A., 2008, 389, 1367
Werner, K., Rauch, T., Kepler, S. O., 2014, 564, A53
Wilson, D. J., Gänsicke, B. T., Koester, D., Raddi, R., Breedt, E., Southworth, J., Parsons, S. G., 2014, 445, 1878
York, D. G., et al., 2000, AJ, 120, 1579
Zhang, Y.-Y., et al., 2013, 146, 34
Zhao, J. K., Luo, A. L., Oswalt, T. D., Zhao, G., 2013, 145, 169
Zuckerman, B., Reid, I. N., 1998, ApJ Lett., 505, L143